

Occupant-Oriented Demand Response with Room-Individual Building Control

Moritz Frahm^a, Thomas Dengiz^b, Philipp Zwickel^a, Heiko Maaß^a, Jörg Matthes^a, Veit Hagenmeyer^a

^aKarlsruhe Institute of Technology, Institute for Automation and Applied Informatics, Eggenstein-Leopoldshafen, Germany

^bKarlsruhe Institute of Technology, Institute for Industrial Production, Karlsruhe, Germany

Abstract

In future energy systems with high shares of renewable energy sources, the electricity demand of buildings has to react to the fluctuating electricity generation in view of stability. As buildings consume one-third of global energy and almost half of this energy accounts for Heating, Ventilation, and Air Conditioning (HVAC) systems, HVAC are suitable for shifting their electricity consumption in time. To this end, intelligent control strategies are necessary as the conventional control of HVAC is not optimized for the actual demand of occupants and the current situation in the electricity grid. In this paper, we present the novel multi-zone controller Price Storage Control (PSC) that not only considers room-individual Occupants' Thermal Satisfaction (OTS), but also the available energy storage, and energy prices. The main feature of PSC is that it does not need a building model or forecasts of future demands to derive the control actions for multiple rooms in a building. For comparison, we use an ideal, error-free Model Predictive Control (MPC) and a conventional hysteresis-based two-point control as upper and lower benchmarks, respectively. We evaluate the three controllers in a multi-zone environment for cooling a building in summer and consider two different scenarios that differ in how much the permitted temperatures vary. The results show that PSC strongly outperforms the conventional control approach in both scenarios with regard to the electricity costs and OTS. It leads to 50 % costs reduction and 15 % comfort improvements while the ideal MPC achieves costs reductions of 58 % and comfort improvements of 29 %. Considering that PSC does not need any building model or forecast, as opposed to MPC, the results support the suitability of our developed control strategy for controlling HVAC systems in future energy systems.

Keywords: multi-zone, thermal building model, RC model, model predictive control, price storage control, rule-based control, occupant behavior, demand response, smart grid

1. Introduction

Buildings consume one-third of global final energy [1]. Almost half of this energy is used by Heating, Ventilation, and Air Conditioning (HVAC) systems to heat or cool buildings [2]. Especially the cooling demand is expected to increase significantly in many parts of the world, as the climate warms on average [3]. In buildings, the energy consumption results from Occupant Behavior (OB) and Occupants' Thermal Satisfaction (OTS) as they interact with the building's energy systems and require comfortable thermal conditions [4]. The energy demand of buildings can be covered with renewable energies in order to reduce greenhouse gas emissions [5].

Flexible electrical loads are pivotal for future energy systems in view of stability to cope with the increasing share of intermittent renewable energy sources like solar and wind energy. For exploiting flexible electric loads in buildings, the HVAC operation can be integrated into Demand Response (DR) programs. DR refers to the change of electricity demand in response to internal or external factors like the price of electricity [6]. In the building sector, electrical HVAC systems, like heat pumps or air conditioners, are suitable for DR. They can exploit existing infrastructure like the building mass or hot water tanks to shift their electricity demand in time [7]. Thus, they can significantly

contribute to better utilization of renewable energy sources and simultaneously help to stabilize the electricity grid. In order to use HVAC systems for DR, optimized control strategies are necessary.

In addition to DR, designing the HVAC operation tailored to the actual occupants' needs could significantly reduce energy use. For example in office spaces, often, not all rooms are occupied. The average occupancy rates of offices are rarely over 60 % [8]. However, the HVAC control in offices usually does not consider the actual occupancy of offices. This leads to unnecessary energy use in unoccupied periods. 56 % of the energy consumed by buildings is used during unoccupied hours and 44 % in occupied hours [9].

For the optimization of HVAC to consider DR and individual OTS, advanced control strategies are required instead of standard thermostats [10], for example Model Predictive Control (MPC) [11] or heuristic control strategies [12]. MPC finds the optimal input trajectory for the HVAC system's control outputs over a future time horizon by solving an optimization problem under consideration of future system dynamics, forecasts, and constraints. Therefore, it requires a dynamic thermal building model and forecasts of OB and weather [13]. The development of models and forecasts can make MPC less practicable and more expensive for real-world applications [11].

Nomenclature

Acronyms

BEV	Battery Electric Vehicle
DR	Demand Response
FMU	Functional Mock-up Unit
HVAC	Heating, Ventilation, and Air Conditioning
KPIs	Key Performance Indicators
MPC	Model Predictive Control
OB	Occupant Behavior
OTS	Occupants' Thermal Satisfaction
PI	Proportional Integral
PMV	Predicted Mean Vote
PPD	Predicted Percentage of Dissatisfied
PSC	Price Storage Control
PV	Photovoltaic
RBC	Rule-based Control
RC	Resistor Capacitor

Parameters

χ_{dis}	discomfort factor
χ_{mod}	heat pump modulation degree
χ_p	price factor
χ_{s_j}	storage factor
Δt	time step in s

ε_h	coefficient of performance of heat pump
ξ_j	allowed deviation buffer in K
C_{i_j}	heat capacity of room air in J K^{-1}
C_{m_j}	heat capacity of heat accumulating medium in J K^{-1}
g_{s_j}	solar heat gain factor in m^2
P_{max}	max. electrical power of heat pump in W
R_{a_j}	resistance between T_{i_j} and T_a in K W^{-1}
R_{i_j}	resistance between T_{i_j} and T_{m_j} in K W^{-1}
S_j	state of thermal charge
y_{max_j}	maximal comfort temperature in $^{\circ}\text{C}$
y_{min_j}	minimal comfort temperature in $^{\circ}\text{C}$
y_{r_j}	reference comfort temperature in $^{\circ}\text{C}$

Variables

\dot{Q}_{h_j}	heat flow of heat pump in W
\dot{q}_s	solar radiation in W m^{-2}
\widehat{F}	empirical distribution function
P_{el}	electrical power of heat pump in W
t	time in s
T_a	ambient temperature in $^{\circ}\text{C}$
T_{i_j}	room air temperature in $^{\circ}\text{C}$
T_{m_j}	heat accumulating medium temperature in $^{\circ}\text{C}$

In contrast, heuristic control strategies are model- and forecast-free heuristic algorithms. They iteratively adjust the power consumption of HVAC systems in order to archive certain goals. In order to do this, they use rule-based control mechanisms and heuristic algorithms that can adapt the HVAC system's heat flows to internal and external signals. Their core advantage is that they do not require a building model to solve an optimization problem [12]. Thus, they are applicable to any building without significant adjustments.

1.1. Related Work

Different control approaches are available in the literature for controlling HVAC systems. Tab. 1 compares the most relevant studies for the present paper. The most significant difference between control strategies is whether they require a model to operate or not.

Most studies in the literature use a model-based approach as they can find the optimal solution of an optimization problem [7]. Especially MPC is popular in the field of DR. Most authors use MPC for controlling HVAC systems, e.g. Maddalena et al. [14], Hu et al. [15], Pedersen et al. [16], Blum et al. [17], Mork et al. [20], and Zwickel et al. [22]. While model-based

approaches generally yield adequate results, they suffer from execution times and require modeling the thermal behavior of a building which is a complex task.

Fewer studies use model-free control strategies. Compared to model-based strategies, the controller design process is significantly simplified, as no building-specific model is required. Model-free control algorithms can be found in the studies of Dengiz et al. [12], Rodriguez et al. [18], Nolting et al. [19], and Michailidis et al. [21]. These approaches are rule-based control mechanisms that are in few cases also combined with a heuristic approach for optimizing an objective function.

In all studies, the objective is to reduce the energy costs while satisfying OTS. Blum et al. [17] additionally consider the provision of ancillary services. Another essential requirement for most of the optimized control approaches is the availability of forecasts. However, most of the model-free approaches do not rely on any forecast.

Our literature review emphasizes the use of control algorithms for multiple zones (see Tab. 1). There are also control approaches in the literature that consider only buildings with one thermal zone (one uniform temperature in the whole building). However, the consideration of multiple zones is closer

Table 1: Comparison of relevant papers studying approaches for demand response of HVAC systems

Literature	Model-free control	Forecast-free control	Multi-zone control	Coupling of multiple buildings possible	Comparison with lower benchmark	Comparison with upper benchmark	Use of measured data
Maddalena et al., 2022 [14]	✗	✗	✓	✗	✓	✓	✓
Hu et al., 2014 [15]	✗	✗	✓	✗	✓	(✓)	✗
Pedersen et al., 2018 [16]	✗	✗	✗	(✓)	✓	✓	✗
Blum et al., 2016 [17]	✗	✗	✓	✓	✗	✓	✗
Dengiz et al., 2019 [12]	✓	✓	✗	✓	✓	✓	✗
Rodríguez et al., 2018 [18]	✓	✓	✓	✗	✓	✗	✗
Nolting et al., 2019 [19]	✓	✓	✗	✗	✓	✗	✗
Mork et al., 2022 [20]	✗	✗	✓	✓	✓	✓	✗
Michailidis et al., 2018 [21]	✓	✗	✓	(✓)	✓	✗	✓
Zwickel et al., 2022 [22]	✗	✗	✗	✓	✗	✓	✗
Present work	✓	✓	✓	(✓)	✓	✓	✓

to the real thermal behavior of buildings and it also increases the complexity of the optimization problem. Another essential feature of control algorithms for DR is their capability of coupling multiple buildings in a coordinated way. While most of the listed studies use a central controller for this, Dengiz et al. [12] define a hybrid control architecture. Zwickel et al. [22] compare central and decentral control approaches for multiple buildings.

To evaluate the performance of the developed control approach, all studies, except for two, use a conventional control approach, like simple rule-based control, hysteresis-based two-point controller, or a Proportional Integral (PI) controller as a lower benchmark. The studies using MPC for controlling the heating or cooling device define their results also as an upper benchmark for the optimization problem, as usually a MPC approach is solved by finding the global optimal solution. Most studies use simulated synthetic data for defining the building model and setting up the simulation. Only Maddalena et al. [14] and Michailidis et al. [21] also use measured data for evaluating the OTS.

1.2. Contribution of this Paper

The main contribution of the present paper is the introduction of a novel heuristic multi-zone control approach, called Price Storage Control (PSC). It combines external factors (e.g. electricity price) and internal factors (temperatures of different zones in the building) to determine when and how much electricity should be consumed for the generation of heat flows. The approach is model-free and does not need any forecasts. To the best of our knowledge, our study is the only one that introduces a novel control approach for buildings with multiple zones that does not need any model or forecasts and that allows for a coordinated coupling of multiple buildings. This is because of its capability to use any external factor for deriving the HVAC control output. Our study is the first that evaluates an introduced model-free and forecast-free control algorithm by using a lower

and upper benchmark that are derived from the use of measured data (see Tab. 1).

To evaluate the PSC control performance in terms of OTS and energy costs, we compare three different control strategies in a multi-zone thermal building model. In the evaluation, we use two scenarios with different degrees of variable room usage. In the base scenario, the temperature range is scheduled between comfort and standby mode. The second scenario also allows room-individual temperature ranges, based on the use case for each room. For comparison, we use an ideal, error-free MPC and a hysteresis-based two-point controller as upper and lower benchmarks.

1.3. Structure of this Paper

We develop and implement three different control strategies and an evaluation environment in the present work. We present the models in Sec. 2, the controllers in Sec. 3, and evaluate them in Sec. 4. Finally, we conclude the evaluation results in Sec. 5.

2. Models

In this section, we present the models that we apply for the evaluation (see Sec. 4) of different control strategies (see Sec. 3). The model-based control strategy, the MPC, also uses the models internally to predict future system dynamics (see Sec. 3.2). The modeling section Sec. 2 is separated into three parts: the model for thermal dynamics of building in Sec. 2.1, for the heat pump in Sec. 2.2, and for OTS in Sec. 2.3.

2.1. Multi-Zone Thermal Building Model

In this section, we develop a multi-zone thermal building model to evaluate room-individual control strategies in Sec. 4. The model applies the Resistor Capacitor (RC) analogy to describe the heat flows between temperature nodes by resistors R and thermal dynamics by capacitors C , as exemplarily shown in Eq. (1).

$$C \frac{dT(t)}{dt} = \dot{Q}_{in}(t) - \dot{Q}_{out}(t) \quad (1)$$

$$\dot{Q}_{xy}(t) = \frac{T_x(t) - T_y(t)}{R}$$

We illustrate our thermal building model structure in Fig. 1. Applying this structure to each room j ($j = 1 \dots n$) results in a decentral multi-zone model [23]. Mathematically, each room is

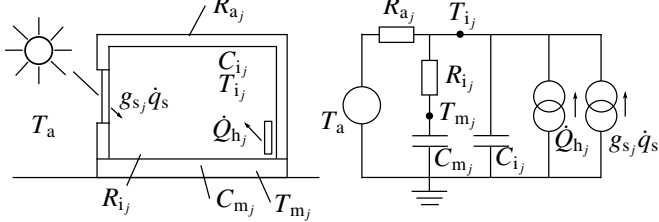


Figure 1: Thermal building model for each room j ($j = 1 \dots n$), obtained from [23] (modified from [24])

thermally defined by the two differential equations Eq. (2) and (3).

$$C_{ij} \frac{dT_{ij}}{dt} = \frac{T_{mj} - T_{ij}}{R_{ij}} + \frac{T_a - T_{ij}}{R_{aj}} + g_{s,j} \dot{q}_s + \dot{Q}_{h,j}, \quad (2)$$

$$C_{mj} \frac{dT_{mj}}{dt} = \frac{T_{ij} - T_{mj}}{R_{ij}}. \quad (3)$$

2.2. Heat Pump Model

The modeled air-source heat pump has a maximum electrical power P_{max} and an energy efficiency ratio ε_h which are both dependent on the ambient temperature. We use the model *AERO SLM 3-11 HGL* from the Austrian heat pump manufacturer *iDM Energiesysteme GmbH* [25] with a supply temperature of the cooling system of 18°C . To calculate the efficiency and the maximum cooling power at every time slot, we use the data from the manufacturer's technical fact sheet and linear interpolation.

The heat pump can modulate its power consumption P_{el} and thus the heat flow \dot{Q}_h with χ_{mod} between 20% and 100%. This leads to the following relation between the heat pump's electrical power P_{el} and the thermal building model's heat pump heat flows:

$$\sum_{j=1}^n |\dot{Q}_{h,j}| = |\dot{Q}_h| = \varepsilon_h \cdot P_{el} = \varepsilon_h \cdot (\chi_{mod} \cdot P_{max}), \quad (4)$$

$$\chi_{mod} \in \{0, [0.2, 1]\}, \quad (5)$$

$$P_{el} = \chi_{mod} \cdot P_{max} \quad (6)$$

2.3. Occupants' Thermal Satisfaction (OTS) Model

In this section, we define the temperature ranges $[y_{min}, y_{max}]$ based on international standards for Occupants' Thermal Satisfaction (OTS) modeling. The three most frequently cited OTS standards are *ASHRAE Standard 55* [26], *ISO 7730:2005* [27], and *EN 16798-1:2019* [28]. These standards are fundamentally

based on the Predicted Mean Vote (PMV) standard scale, which was first introduced by Fanger's model [29].

The PMV is a static model evaluated from a large group of people with a given combination of thermal environmental and personal parameters. These parameters include metabolic activity, clothing, air temperature, radiant temperature, air velocity, and relative humidity. In a survey, occupants express their thermal sensations on a scale from -3 (too cold) to +3 (too warm), where 0 is optimum. Fanger also developed an equation that relates the PMV to the Predicted Percentage of Dissatisfied (PPD). The standard OTS guidelines aim for a PMV from -0.5 to +0.5 (OTS level II, see Tab. 2). The OTS level can also be within closer or wider PMV boundaries, e.g. ± 0.2 for level I or ± 0.7 for level III. Wider temperature limits result in lower energy consumption of HVAC systems.

Based on these OTS levels in Tab. 2, we calculate the corresponding lower y_{min} and upper y_{max} temperature limits that are required for Eq. (21). For the calculation of the temperature limits, we use the CBE Thermal Comfort Tool [30] with EN-16798 standard and summer clothing. In this tool, we set the mean radiant temperature equal to the air temperature T_i . This implies the assumption that the operative temperature is close to the air temperature. For more information about the operative temperature, we refer to our previous work [31]. The resulting temperature limits for different levels of OTS are presented in Tab. 2.

Table 2: OTS categories, obtained from CBE Thermal Comfort Tool [30] with EN-16798 and summer clothing

OTS level	PMV	PPD	y_{min} in $^\circ\text{C}$	y_{max} in $^\circ\text{C}$
I	± 0.2	< 6%	25.6	26.6
II	± 0.5	< 10%	24.8	27.4
III	± 0.7	< 15%	24.2	27.9

Based on the temperature limits, we calculate the reference comfort temperature y_r in Eq. (7). This reference temperature is required for the controller design of the PSC in Sec. 3.1.

$$y_r = \frac{y_{min_j} + y_{max_j}}{2} \quad (7)$$

3. Control Strategies

This section describes the development of three different control strategies: PSC in Sec. 3.1, MPC in Sec. 3.2, and hysteresis-based two point control in Sec. 3.3. The objective is to minimize the electricity costs given by a time-variable electricity price and to maximize the OTS. While we develop the PSC as a novel control methodology for occupant-oriented demand-response with room-individual building control, the MPC and hysteresis-based two-point controller are used as upper and lower benchmarks, respectively. The MPC was implemented in Python with a prediction horizon of 16 hours and solved using Gurobi. Also, PSC and the two-point controller are implemented in Python.

In general, the three control strategies are applicable to cooling or heating. For both cases, we use the generic term *heat flows*. A heat flow is the rate of net heat energy transfer between hot and cold sides and can be positive or negative for heating or cooling, respectively.

3.1. Price Storage Control (PSC)

The PSC is a heuristic control algorithm for modulating HVAC or heat pump heat flows \dot{Q}_{h_j} in a multi-zone building. It essentially consists of 4 steps which it executes in every time slot.

1. Determine the price factor $\chi_p(t)$ based on [12].
2. Determine the storage factor $\chi_s(t)$.
3. Calculate the modulation degree χ_{mod} using the price factor $\chi_p(t)$ and the storage factor $\chi_s(t)$.
4. Distribute the generated heat flow to the different rooms of the multi-zone building.

Price Factor

To obtain the price factor χ_p , the algorithm calculates the empirical distribution function $\widehat{F}(p)$ for the future electricity prices $p(t)$ of the next 24 hours at the beginning of each day. We assume that we have an electricity tariff with predetermined prices for the next 24 hours (for more information see Section 4.1.1). At every time slot of the day, the value of the $\widehat{F}(p)$ is calculated for the current price $p(t)$. The calculation of the empirical distribution function $\widehat{F}(p)$ is illustrated in Fig. 2, exemplarily for one day. $\widehat{F}(p)$ quantifies the share of electricity prices for the current day that have a lower or equal value compared to the price p of the current time slot. PSC sets the price factor at time slot t as in Eq. (8). A low price results in a high price factor (due to a high value of $\widehat{F}(p)$) and vice versa.

$$\chi_p(t) = 1 - \widehat{F}(p(t)) \quad (8)$$

Storage Factor

For the calculation of the storage factor $\chi_s(t)$, the state of thermal charge $S_j(t)$ from Eq. (9) is needed for each room. The state of thermal charge $S_j(t)$ quantifies the “stored” temperature room individually and results in values between 0 and 1. Although the PSC method is applicable for heating or cooling heat flows, we explain this method exemplarily for the cooling case in the following.

$$S_j(t) = \frac{y_{r_j} + \xi_j - T_{i_j}(t - \Delta t)}{\xi_j} \quad (9)$$

If the temperature of the room j from the last time slot $T_{i_j}(t - \Delta t)$ is lower than the reference temperature y_{r_j} the state of thermal charge $S_j(t)$ is set to 1. This means that the thermal storage of this room is full and there is no necessity for applying heat flows to the room ¹.

¹As we are considering cooling in the present work it has to be noted that full thermal storage, in this case, means, that the temperature in the room is low and thus the room already has enough “cooling energy”.

If the temperature of the room is higher than the reference comfort temperature y_{r_j} plus an allowed deviation buffer ξ_j , for sufficiently high OTS, the state of thermal charge $S_j(t)$ is set to 0. In the cooling case, this results in empty thermal storage as the temperature in the room is too high.

For every room temperature that is between the reference temperature and the upper OTS limit ($y_{r_j} + \xi_j$), the algorithm uses Eq. (9) to calculate the state of thermal charge $S_j(t)$ of room j ($j = 1 \dots n$). The reference temperature for every room y_{r_j} is calculated as in Eq. (7). This value depends on the investigated scenarios (see Sec. 4) ².

After having determined the state of thermal charge $S_j(t)$ for every room n , the algorithm calculates the storage factor $\chi_s(t)$ by using Eq. (10). If the temperatures in the different rooms are close to the lower limit, their corresponding state of thermal charge will be high resulting in a low storage factor $\chi_s(t)$ and vice versa.

$$\chi_s(t) = 1 - \frac{\sum_{j=1}^n S_j(t)}{n} \quad (10)$$

Modulation Degree of the HVAC system

The third step of the algorithm is the calculation of the heat pump’s modulation degree and thus the heat flow and the electrical power using Eq. (11). The modulation degree $\chi_{\text{mod}}(t)$ results from the multiplication of the price factor χ_p and storage factor χ_s . Because both factors can have values between 0 and 1, the modulation degree $\chi_{\text{mod}}(t)$ likewise varies between 0 and 1. We choose a multiplication of the two factors instead of a weighted sum as this leads to better results in our case studies. Based on the modulation degree, Eq. (4)) and Eq. (5) calculates the generated heat flows and electrical power.

$$\chi_{\text{mod}}(t) = \chi_p(t) \cdot \chi_s(t) \quad (11)$$

Two factors influence the heat pump power output. A high electricity price leads to a low price factor which leads to low values of the modulation degree. This results in low electricity consumption at that time. On the contrary, a low price leads to a high price factor which incentivises the heat pump to cool down the room. This is desired as we want to generate heat flows when the electricity prices are low.

Next to the price factor, the storage factor impacts the generated heat flows and thus consumed electricity. If the temperatures in the rooms are generally low, the storage factor has low values due to the high values of the state of thermal charge $S_j(t)$. A low storage factor leads to low power consumption and vice versa. This is also a desired property of the control algorithm. If the room temperatures are already low, there is no urgent need for cooling whereas high room temperatures tend to lead to higher generation of heat flow using the PSC algorithm.

Distribution of Heat Flows

In the final step, the algorithm distributes the generated heat flows to the different rooms j ($j = 1 \dots n$). To do this, the

²For this internal parameter of the algorithm, a buffer value of $\xi_j = 2$ K yields adequate results in the present work.

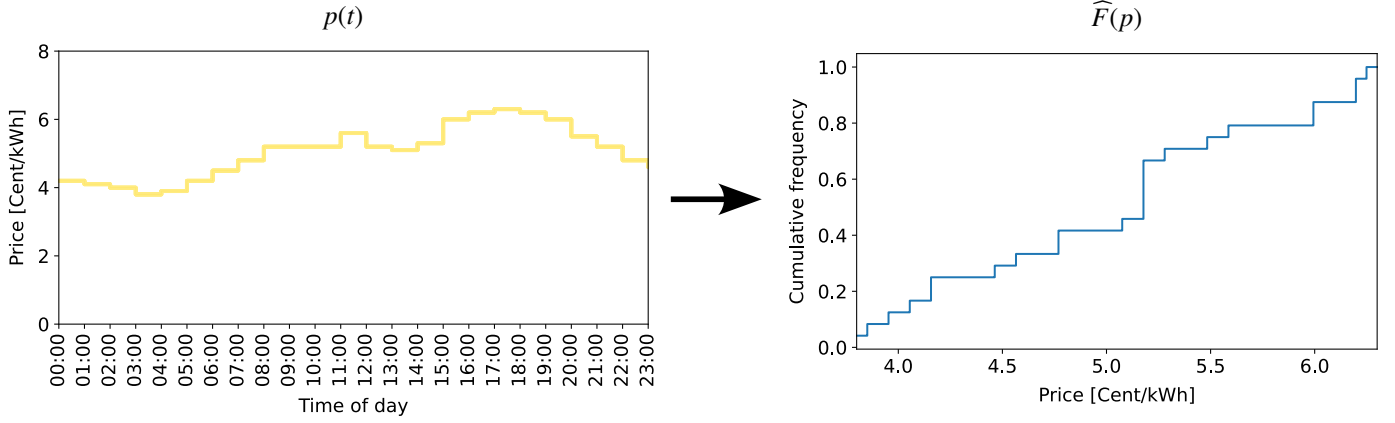


Figure 2: Empirical distribution function of the electricity prices

caused thermal discomfort of each room $d_{c_j}(t)$ due to possibly too high temperatures is determined. If the temperature of a room from the previous time slot $T_{i_j}(t - \Delta t)$ is higher than the upper temperature limit y_{\max_j} , Eq. (12) and Eq. (14) quantify the caused discomfort of the room j and the total caused discomfort $d_{c,\text{total}}(t)$ from Eq. (13).

$$d_{c_j}(t) = T_{i_j}(t - \Delta t) - y_{\max_j} \quad (12)$$

$$d_{c,\text{total}}(t) = \sum_{j=1}^n d_{c_j}(t) \quad (13)$$

Based on the total caused discomfort $d_{c,\text{total}}(t)$ the PSC algorithm distributes the generated heat flows \dot{Q}_h of time t to each room j with \dot{Q}_{h_j} using Eq. (14). This mechanism assures that especially rooms that have high temperatures, get more heat flow (cooling) than rooms with less need for cooling. If the heat pump generates heat flows although no room has violated its temperature boundaries in the last time slot, it equally distributes the generated heat flows to every room.

$$\dot{Q}_{h_j}(t) = \frac{d_{c_j}(t)}{\sum_{j=1}^n d_{c_j}(t)} \cdot \dot{Q}_h(t) \quad (14)$$

Overall, PSC executes the four mentioned steps for every time slot of the day while updating the empirical distribution function of the prices at the beginning of each day.

3.2. Model Predictive Control (MPC)

In contrast to PSC, MPC requires a model which is obtained by restructuring the thermal building model from Sec.2 into state-space notation. The resulting equations for n rooms are

$$\begin{aligned} \dot{x}(t) &= f(x(t), u(t), z(t)) = Ax(t) + Bu(t) + Ez(t), \\ y(t) &= g(x(t)) = Cx(t) \end{aligned} \quad (15)$$

where x describes the temperature states of the buildings' air temperatures (T_{i_j}) and thermal masses (T_{m_j}), u the control inputs (\dot{Q}_{h_j}), z the measurable disturbances (\dot{q}_s , T_a), and y the

outputs (T_{i_j}) with

$$\begin{aligned} x &= (T_{i_1} \ T_{m_1} \ T_{i_2} \ T_{m_2} \ \dots \ T_{i_n} \ T_{m_n})^\top, \\ u &= (\dot{Q}_{h_1} \ \dot{Q}_{h_2} \ \dots \ \dot{Q}_{h_n})^\top, \\ z &= (\dot{q}_s \ T_a)^\top, \\ y &= (T_{i_1} \ T_{i_2} \ \dots \ T_{i_n})^\top. \end{aligned} \quad (16)$$

Given the heat pump model (see Eq. (4) and Eq. (5)) and the control model (Eq. (15)), we formulate the optimization problem with a prediction horizon of N time steps, which must be solved at each sampling instant t , based on [22] as

$$\min \sum_{k=t}^{t+N-1} l(k, \chi_{\text{dis}}(k|t), P_{\text{el}}(k|t)) \quad (17a)$$

subject to $\forall k \in [0, N - 1]$:

$$x(k+1|t) = A_d x(k|t) + B_d u(k|t) + E_d z(k|t) \quad (17b)$$

$$y(k|t) = C_d x(k|t) \quad (17c)$$

$$x(0|t) = x(t), \quad (17d)$$

$$P_{\text{el}}(k|t) = \chi_{\text{mod}}(k|t) \cdot P_{\text{max}}(k), \quad (17e)$$

$$\chi_{\text{mod}}(k|t) \in \{0, [0.2, 1]\}, \quad (17f)$$

$$u(k|t) \in \mathcal{U}, y(k|t) \in \mathcal{Y} \quad (17g)$$

where $l(k, \cdot, \cdot)$ is the stage-cost, (17b) and (17c) are the discrete-time control model, (17d) is the initial condition, and (17e) and (17f) are the heat pump model. $x(t)$ is typically measured at the time t , and \mathcal{U} as well as \mathcal{Y} are input and output constraint sets (see (17g)). The k -step ahead prediction for the states, inputs, disturbances, outputs, discomfort factor, heat pump modulation degree, and electric power, based on the current initial condition are denoted by $x(k|t)$, $u(k|t)$, $z(k|t)$, $y(k|t)$, $\chi_{\text{dis}}(k|t)$, $\chi_{\text{mod}}(k|t)$, and $P_{\text{el}}(k|t)$, respectively.

We consider the following stage cost

$$l(k, \chi_{\text{dis}}(k), P_{\text{el}}(k)) = \lambda \left(\sum_{j=1}^n \chi_{\text{dis}_j}(k) \right) + (1-\lambda) (P'_{\text{el}}(k) p'(k)) \quad (18)$$

where $\lambda \in [0, 1]$ is a user-defined weighting coefficient and $p(k)$, $k \in t : t + N - 1$ is a time-dependent price signal (future

electricity prices). $P'_{el}(k|t)$ and $p'(k)$ are the min-max normalization of $P_{el}(k|t)$ and $p(k)$ ³, respectively, calculated as

$$\begin{aligned} P'_{el}(k) &= \frac{P_{el}(k) - \min\{P_{el}\}}{\max\{P_{el}\} - \min\{P_{el}\}}, \\ p'(k) &= \frac{p(k) - \min\{p\}}{\max\{p\} - \min\{p\}}. \end{aligned} \quad (19)$$

Furthermore, the control inputs u are limited to cooling with the maximum total power constraint by the heat pump model, as formulated in Eq. (4), which leads to

$$\mathcal{U} = \left\{ u \in \mathbb{R}^n \mid (\forall j \in [1, n] : u_j \leq 0) \wedge \sum_{j=1}^n |u_j| = \varepsilon_n \cdot P_{el} \right\}. \quad (20)$$

In addition, the control outputs should meet predefined time-variant temperature ranges $[y_{\min_j}, y_{\max_j}]$ for each room j . This leads to the following soft constraints:

$$\begin{aligned} \mathcal{Y} = \left\{ y \in \mathbb{R}^n \mid (\forall j \in [1, n] : y_{\min_j} - \chi_{\text{dis}_j} \leq y_j \leq y_{\max_j} + \chi_{\text{dis}_j}) \right. \\ \left. \wedge \chi_{\text{dis}_j} \geq 0 \right\}. \end{aligned} \quad (21)$$

3.3. Hysteresis-based Two-point Controller

The hysteresis-based two-point control serves as the lower benchmark for the evaluation. This is a conventional control strategy for cooling (or heating) devices that cools down a room until a lower temperature limit. Afterward, the device switches off and waits until the temperature in the room has reached an upper limit. This triggers the control system to start cooling down again. We use an adaptive hysteresis that uses the upper and lower temperature limits $[y_{\min_j}(t), y_{\max_j}(t)]$ depending on the scenarios. These predefined temperature limits for OTS are described in the evaluation scenarios in Sec. 4.1.2.

4. Evaluation

In this section, we compare the control algorithms and describe the used evaluation environment. First, we introduce the used data, scenarios, and metrics in Sec. 4.1. Then, we present the results in Sec. 4.2, discuss them in Sec. 4.3, and show limitations in Sec. 4.4

4.1. Data, Scenarios, and Metrics

4.1.1. Data

We evaluate the control strategies by using weather data during the summer of 2022, obtained from a weather station on an experimental building [32]. This building is located in the *KIT EnergyLab 2.0* (Karlsruhe, Germany), and is presented in Fig. 3a. It has a design similar to a single-family home and is used as an office space. For the evaluation, we use the measurements of the weather station (the solar radiation \dot{q}_s and the ambient temperature T_a) over a period of 13 weeks (05/30/2022 –

08/22/2022). Due to measurement gaps, we had to sort out three weeks (8th, 10th, and 13th week) and could only use the remaining ten weeks. We use the ten weeks of data in time steps of $\Delta t = 15$ min. For the variable electricity tariff, we use the data of the day-ahead market in Germany from the *ENTSO-E Transparency Platform* [33]. The price is different for every hour of the day and we assume that these prices are directly forwarded to the customers.

In Sec. 4.2, we evaluate the control algorithms from Sec. 3 on an evaluation environment that is illustrated in Fig. 3. While the evaluation environment is inspired by the building design in Fig. 3a, the floor plan in Fig. 3b is generated artificially. The floor plan illustrates the different temperature demands of the rooms in Tab. 3 and 4. In the present work, we explicitly focus on the evaluation of control strategies instead of model parameter estimation from measurements. For more information about parameter identification, we refer to our previous work [23]. For the results in Sec 4.2, the model parameters of the model in Sec. 2 are based on parameters from the literature [24] and scaled to consider different room sizes. The used model and parameters can be obtained from GitHub (as a Modelica file *.mo* and as a Functional Mock-up Unit (FMU) *.fmu*)⁴.

4.1.2. Scenarios

For the evaluation of the control algorithms, we consider two scenarios, namely (a) *base scenario* and (b) *multi-zone adaptive scenario*. The scenarios differ by their variability of temperature ranges $[y_{\min_j}(t), y_{\max_j}(t)]$. The base scenario applies the same ranges for all rooms, while the second allows individual occupancy profiles. The temperature ranges are presented in Tab. 3 and 4 and applied for each day. Despite the office scenario, we do not differentiate between the different days, e.g. between weekdays and weekends, to simplify the evaluation.

(a) Base scenario: We use two different control modes in the base scenario (see Tab. 3): a comfort mode and a standby mode (inspired by Peng et al. [34]). We apply the comfort mode during working hours from 8AM to 5PM and the standby mode else.

Table 3: (a) Base scenario, room air temperatures in °C

Period	Room	1	2	3	4	5
8AM to 5PM	y_{\min_j}	24.8	24.8	24.8	24.8	24.8
	y_{\max_j}	27.4	27.4	27.4	27.4	27.4
else	y_{\min_j}	16.0	16.0	16.0	16.0	16.0
	y_{\max_j}	30.0	30.0	30.0	30.0	30.0

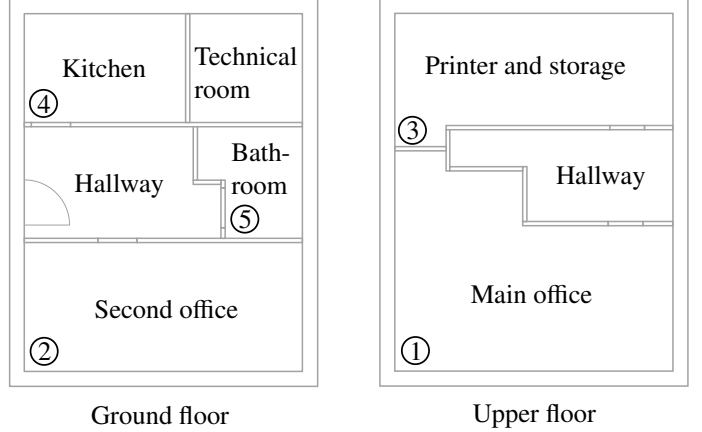
All rooms j ($j = 1 \dots 5$) apply the same modes during the entire evaluation in the base scenario. As a result, the temperature ranges $[y_{\min_j}(t), y_{\max_j}(t)]$ in Tab. 3 are all equal over the different rooms. In contrast, the second scenario uses different modes in different rooms, depending on the use case of each room.

³In the present study, we apply $\min\{P_{el}\} = 0$ W, $\max\{P_{el}\} = 3500$ W, $\min\{p\} = 6.9$ Cent/kWh, and $\max\{p\} = 58.1$ Cent/kWh.

⁴<https://github.com/Occupant-Oriented-Demand-Response/Control-Results>



(a) Experimental building with a design similar to a single-family home



(b) Floor plan

Figure 3: Evaluation environment

(b) Multi-zone adaptive scenario: The temperature ranges $[y_{\min_j}(t), y_{\max_j}(t)]$ in all rooms j ($j = 1 \dots 5$) can be different (see Tab. 4). In addition to the comfort and standby mode, we also use an eco mode that schedules the reference temperature by 2 K (+2 K/-2 K for cooling/heating) difference compared to the comfort mode [34]. This eco mode saves energy compared to the comfort mode and also enables fast re-cooling / re-heating compared to the standby mode. In addition, the eco mode can save energy in rooms that are less frequently used than office rooms, e.g. bathrooms or kitchens.

Table 4: (b) Multi-zone adaptive scenario, room air temperatures in °C

Period	Room	1	2	3	4	5
8AM to 12AM	y_{\min_j}	24.8	24.8	22.8	22.8	22.8
	y_{\max_j}	27.4	27.4	29.4	29.4	29.4
12AM to 1PM	y_{\min_j}	22.8	22.8	22.8	24.8	22.8
	y_{\max_j}	29.4	29.4	29.4	27.4	29.4
1PM to 5PM	y_{\min_j}	24.8	22.8	22.8	22.8	22.8
	y_{\max_j}	27.4	29.4	29.4	29.4	29.4
else	y_{\min_j}	16.0	16.0	16.0	16.0	16.0
	y_{\max_j}	30.0	30.0	30.0	30.0	30.0

In the multi-zone adaptive scenario (see Tab. 4), we let the control operate with a high focus on OTS in occupied rooms and energy saving in unoccupied. Therefore, we use the comfort mode in the offices (rooms 1 and 2) during working hours and the kitchen (room 4) during lunch breaks from 12AM to 1PM. In this scenario, the first office (room 1) is used over the entire working day, except lunch break, and the second office (room 2) only from 8AM to 12AM (part-time job). The bathroom (room 5) and storage (room 3) should be operated in eco mode during working hours (8AM to 5PM).

4.1.3. Metrics

We use two Key Performance Indicators (KPIs) to evaluate (i) how accurately a controller meets the desire OTS and (ii) how much energy the control strategy therefore consumes.

Mathematically we define the KPIs as the weekly costs $c_{m, \text{week}}$ in Eq. (22) and mean weekly discomfort $d_{m, \text{week}}$ in Eq. (23),

$$c_{m, \text{week}} = \sum_{k=1}^M \left(p(k) \int_k P_{el}(k) dt_k \right) \quad (22)$$

$$d_{m, \text{week}} = \frac{1}{M} \left(\sum_{k=1}^M \sum_{j=1}^n d_{c_j}(k) \right). \quad (23)$$

The KPIs consider energy costs and OTS during each time-step k for all time steps $M = 672$ of each week. The energy costs $c_{m, \text{week}}$ depend on a dynamic energy tariff $p(k)$ and the consumed electric power $P_{el}(k)$. The discomfort $d_{m, \text{week}}$ evaluates the discomfort $d_{c_j}(k)$ of the actual room temperature from the allowed OTS range. This permitted temperature range is time-variant, depending on room-individual usage/attendance profiles, as introduced in the scenarios in Sec. 4.1.2.

Both KPIs are competing, which means when one is improved, the other is usually deteriorating. It is the objective to minimize both KPIs simultaneously, to have low costs and low discomfort.

4.2. Results

We present the results of the three different control algorithms, MPC (ideal and error-free), PSC, and hysteresis-based two-point controller (see Sec. 3), in Fig. 4 and A.5. The overall results for both scenarios over the entire evaluation period of ten weeks can be obtained from Fig. 4. Fig. A.5 illustrates the dynamic response of the thermal building model to the three applied control strategies, exemplarily for the base scenario during one week.

Control Results for One Week

Fig. A.5 illustrates the dynamic behavior of the three controllers, MPC, PSC, and hysteresis-based two-point controller, on the multi-zone thermal building model. The x-axis uses the time in days for one week in June/July 2022. On the y-axis, we present the air temperatures T_i in °C for five rooms ($j = 1 \dots 5$) and three control strategies. The blue area shows the permitted

temperature ranges for the air temperatures $[y_{\min_j}(t), y_{\max_j}(t)]$. The bottom y-axes present the controlled variable P_{el} , the disturbance variables T_a and \dot{q}_s , and the dynamic electric price function p .

The control characteristics of the three controllers are distinguishable, although, for all controllers, the controlled variable P_{el} of the heat pump operates only in three of seven days noticeably (06-29, 06-30, and 07-03). In general, the temperature trajectories controlled by MPC and PSC are more similar than those controlled by the hysteresis-based two-point controller. The MPC cools most frequently but at a lower power P_{el} . In a few cases, the MPC exceeds the upper temperature limits, e.g. on the 06-30. Therefore, the MPC meets temperature ranges more adequately on the next day (07-01), where the temperatures of the PSC and hysteresis-based two-point controller are too low.

Overall Results for Ten Weeks

We perform evaluations for the three controllers in two scenarios over ten different weeks and summarize the results in Fig. 4. On the y-axis in Fig. 4, we visualize the two KPIs, the *mean weekly costs* ("costs") and the *mean discomfort* ("discomfort") from Eq. (22) and (23). The results are shown for the two scenarios, the (a) *base scenario* and the (b) *multi-zone adaptive scenario*, where (a) and (b) are based on the temperature ranges in Tab. 3 and 4, respectively.

When evaluating the three control strategies in Fig. 4, the MPC and PSC show superior results in terms of costs and discomfort, compared to the hysteresis-based two-point controller. In both scenarios, the MPC and PSC have lower discomfort and approximately half the costs of the hysteresis-based two-point controller (e.g. in (a) from 2.18 to 1.08 or 1.18).

The performance of the MPC depends more on the evaluated scenario (a) vs. (b) than for the other two controllers. In the base scenario, The MPC and PSC have a similar overall performance (1.18 vs. 1.08 costs and 0.52 vs. 0.59 discomfort). In contrast, in the multi-zone adaptive scenario, the MPC outperforms the PSC with 38.5% lower costs (from 1.09 to 0.67) and also lower discomfort (from 0.19 to 0.13).

In summary, we obtain the highest overall performance regarding costs and discomfort with the MPC and PSC, while the hysteresis-based two-point controller shows the lowest performance. The performance difference between MPC and PSC varies depending on the evaluation scenario. In the (a) *base scenario*, the MPC and PSC have similar control results, while in the (b) *multi-zone adaptive scenario*, the MPC outperforms the PSC with 38.5% lower costs and also lower discomfort.

4.3. Discussion

The results in Sec. 4.2 evaluate the performance of the PSC by comparison with the upper and lower benchmarks using ideal, error-free MPC and hysteresis-based two-point controller, respectively. Overall, the control performance of the PSC is significantly superior to the hysteresis-based two-point controller and close to the ideal MPC. In the following, we discuss the differences in control performance.

The three controllers differ in their complexity and how much knowledge about future system behavior they require. The hysteresis-based two-point controller uses only minimal and maximal temperatures $[y_{\min_j}(t), y_{\max_j}(t)]$ without any forecasts or models. When a maximal temperature is reached, it cools over a defined period. The PSC, on the other hand, tries to meet a reference temperature that is in the middle of the minimal and maximal ranges. The PSC requires knowledge about the temperature ranges, but also about the energy tariff and the heat pump modulation. Exploiting this knowledge reduces the energy costs of the PSC compared to the hysteresis-based two-point controller because the PSC can apply cooling during periods of low energy prices.

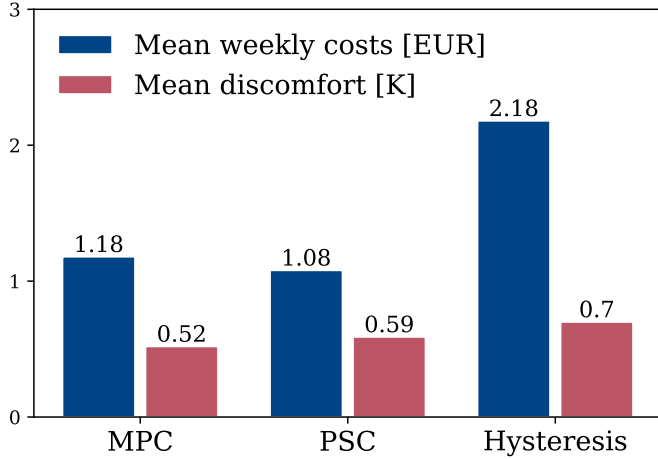
The MPC uses the largest amount of available information, which increases its performance accordingly. It does not only use temperature ranges, energy tariffs, and heat pump modulation. In addition, the MPC needs a thermal building model and weather forecasts. With that internal control model and the forecasts, the MPC can predict future system behavior in advance and schedule the cooling load optimally. As a result, MPC outperforms the PSC when high variations in the temperature ranges $[y_{\min_j}(t), y_{\max_j}(t)]$ occur, as in the (b) *multi-zone adaptive scenario*. The MPC exploits the knowledge about thermal storage inside the building, which enables finding an optimal cooling trajectory.

The PSC is suitable for tracking a reference temperature when fewer variations in the temperature ranges occur. In the (a) *base scenario*, the PSC and MPC show similarly high performance. It should be noted that in the base scenario, a major part of the discomfort results from a too-cold temperature, instead of a too-warm one. None of the three controllers was allowed to heat the building. Especially in the morning periods, the low ambient temperatures make it challenging for the controllers to meet warm enough thermal conditions in the building. The MPC can only mitigate temperatures that are too low by allowing temperatures that are too warm at other times (see Fig. A.5, 06-30 and 07-01). Overall, the MPC cannot show its advantage as an optimum controller to its best advantage in the base scenario.

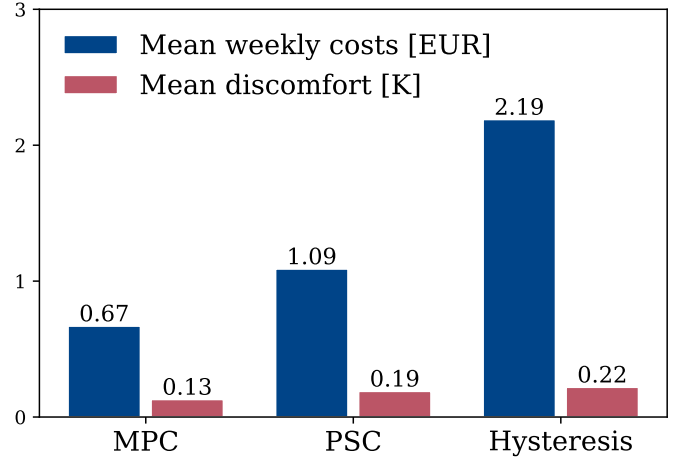
In summary, the controllers perform as expected where a higher complexity and use of more information improve the control quality. While the PSC outperforms the hysteresis-based two-point controller, the differences between PSC and ideal MPC are much smaller. On the one hand, the MPC has a superior performance in one of the two scenarios. On the other hand, the MPC is significantly more complex to design, requiring a thermal model for each room and a forecast, which we both assumed to be error-free for our case study. Compared to the conventional hysteresis-based two-point controller, PSC leads to a reduction of the two combined criteria costs and discomfort of 44% (50% costs reduction and 15% comfort improvements) while the MPC achieves combined improvements of 53% (58% cost reduction and 29% comfort improvements).

4.4. Limitations

The evaluation of control strategies in this work is based on simulation results, which can neglect several effects from



(a) Base scenario evaluation



(b) Multi-zone adaptive scenario evaluation

Figure 4: Control results of three controllers, evaluated in two different scenarios (a) and (b)

the real application. The control strategies are performed on a multi-zone thermal building model instead of a real building. The model parameters are based on literature values instead of identification from parameter identification. The model and weather forecasts of the MPC are assumed as error-free.

The evaluation is limited to a cooling scenario of a single building. Weather data is used for ten weeks during summer in Karlsruhe, Germany. The cooling demand in Germany is lower than in other regions of the world. A heating scenario is not investigated. The evaluated scenarios consider no Photovoltaic (PV), battery, Battery Electric Vehicle (BEV), or thermal water storage in the optimization.

5. Conclusion

In this study, we investigate how a novel multi-zone Price Storage Control (PSC) can provide Demand Response (DR) while considering room-individual Occupants' Thermal Satisfaction (OTS) without using a thermal building model and weather forecasts. Therefore, we develop three different control strategies, a multi-zone evaluation environment, and two different scenarios to compare the controllers. We compare the PSC with an ideal, error-free Model Predictive Control (MPC) and hysteresis-based two-point controller as upper and lower benchmarks, respectively.

The ideal MPC and PSC achieve higher control performance than the hysteresis-based two-point controller in terms of energy costs and mean discomfort. The PSC leads to a reduction of both criteria combined of 44 % while the MPC achieves improvements of 53 %. Under consideration that the PSC requires no models and no forecasts, this control strategy seems especially beneficial for real-world control applications. Our developed control approach is easy to implement and can be used for every building without large-scale adjustments. Further, it can include other external signals in its decision-making like the load of the electricity grid or a generation signal of renewable energy sources. Thus, it can contribute to balancing electricity

demand and supply and lead to better utilization of renewable energy sources in future energy systems.

In future work, we want to apply the developed control strategy to a real-world application. For the MPC real-world application, we need to perform parameter identification and design a state estimator. For a more realistic scenario, we plan to include more relevant components into the optimization, e.g. thermal water storage, Photovoltaic (PV) self-production and -consumption, and batteries. Finally, we plan to evaluate the controller in a heating scenario.

Data Availability

We added the following supplementary materials to an open-source online repository on GitHub:

- results of the three control strategies for all individual weeks in both scenarios,
- used input data for the electricity price and weather data,
- commented Python code of the three control strategies.

<https://github.com/Occupant-Oriented-Demand-Response/Control-Results>.

Acknowledgment

This work was conducted within the project FlexKälte, funded by the German Federal Ministry for Economic Affairs and Climate Action (BMWK). The authors would like to thank their colleagues from the Energy Lab 2.0 and the Institute for Automation and Applied Informatics (IAI) for all the fruitful discussions and collaborations.

Appendix A. Control Results for One Week

The control results for one week, as discussed in Sec. 4.2, are presented in Fig. A.5.

References

- [1] IEA, Buildings - a source of enormous untapped efficiency potential, (accessed: 15.12.2022) (2022). URL <https://www.iea.org/topics/buildings>
- [2] L. Yang, H. Yan, J. C. Lam, Thermal comfort and building energy consumption implications – a review, *Applied Energy* 115 (2014) 164–173. doi:<https://doi.org/10.1016/j.apenergy.2013.10.062>.
- [3] R. Mutschler, M. Rüdüsili, P. Heer, S. Eggimann, Benchmarking cooling and heating energy demands considering climate change, population growth and cooling device uptake, *Applied Energy* 288 (2021) 116636. doi:<https://doi.org/10.1016/j.apenergy.2021.116636>.
- [4] T. Hong, D. Yan, S. D'Oca, C. fei Chen, Ten questions concerning occupant behavior in buildings: The big picture, *Building and Environment* 114 (2017) 518–530. doi:<https://doi.org/10.1016/j.buildenv.2016.12.006>.
- [5] F. M. Vieira, P. S. Moura, A. T. de Almeida, Energy storage system for self-consumption of photovoltaic energy in residential zero energy buildings, *Renewable Energy* 103 (2017) 308–320. doi:<https://doi.org/10.1016/j.renene.2016.11.048>.
- [6] M. H. Albadi, E. F. El-Saadany, Demand response in electricity markets: An overview, in: 2007 IEEE Power Engineering Society General Meeting, 2007, pp. 1–5. doi:10.1109/PES.2007.385728.
- [7] T. Dengiz, Optimization approaches for exploiting the load flexibility of electric heating devices in smart grids, Ph.D. thesis, Karlsruhe Institut für Technologie (KIT) (2021). doi:10.5445/IR/1000131495.
- [8] A. Mahdavi, A. Mohammadi, E. Kabir, L. Lambava, Occupants' operation of lighting and shading systems in office buildings, *Journal of Building Performance Simulation* 1 (1) (2008) 57–65. doi:10.1080/19401490801906502.
- [9] O. Masoso, L. Grobler, The dark side of occupants' behaviour on building energy use, *Energy and Buildings* 42 (2) (2010) 173–177. doi:<https://doi.org/10.1016/j.enbuild.2009.08.009>.
- [10] P. H. Shaikh, N. B. M. Nor, P. Nallagownden, I. Elamvazuthi, T. Ibrahim, A review on optimized control systems for building energy and comfort management of smart sustainable buildings, *Renewable and Sustainable Energy Reviews* 34 (2014) 409–429. doi:<https://doi.org/10.1016/j.rser.2014.03.027>.
- [11] J. Drgoña, J. Arroyo, I. Cupeiro Figueroa, D. Blum, K. Arendt, D. Kim, E. P. Ollé, J. Oravec, M. Wetter, D. L. Vrabie, L. Helsen, All you need to know about model predictive control for buildings, *Annual Reviews in Control* 50 (2020) 190–232. doi:10.1016/j.arcontrol.2020.09.001.
- [12] T. Dengiz, P. Jochem, W. Fichtner, Demand response with heuristic control strategies for modulating heat pumps, *Applied Energy* 238 (2019) 1346–1360. doi:<https://doi.org/10.1016/j.apenergy.2018.12.008>.
- [13] M. Frahm, P. Zwickel, J. Wachter, F. Langner, P. Strauch, J. Matthes, V. Hagenmeyer, Occupant-Oriented Economic Model Predictive Control for Demand Response in Buildings, in: 13th ACM International Conference on Future Energy Systems, e-Energy'22, Association for Computing Machinery, 2022. doi:10.1145/3538637.3538864.
- [14] E. T. Maddalena, S. A. Müller, R. M. dos Santos, C. Salzmann, C. N. Jones, Experimental data-driven model predictive control of a hospital hvac system during regular use, *Energy and Buildings* 271 (2022) 112316. doi:<https://doi.org/10.1016/j.enbuild.2022.112316>.
- [15] J. Hu, P. Karava, A state-space modeling approach and multi-level optimization algorithm for predictive control of multi-zone buildings with mixed-mode cooling, *Building and Environment* 80 (2014) 259–273. doi:<https://doi.org/10.1016/j.buildenv.2014.05.003>.
- [16] T. H. Pedersen, S. Petersen, Investigating the performance of scenario-based model predictive control of space heating in residential buildings, *Journal of Building Performance Simulation* 11 (4) (2018) 485–498. doi:10.1080/19401493.2017.1397196.
- [17] D. H. Blum, N. Xu, L. K. Norford, A novel multi-market optimization problem for commercial heating, ventilation, and air-conditioning systems providing ancillary services using multi-zone inverse comprehensive room transfer functions, *Science and Technology for the Built Environment* 22 (6) (2016) 783–797. doi:10.1080/23744731.2016.1197718.
- [18] L. Romero Rodríguez, J. Sánchez Ramos, S. Álvarez Domínguez, U. Eicker, Contributions of heat pumps to demand response: A case study of a plus-energy dwelling, *Applied Energy* 214 (2018) 191–204. doi:<https://doi.org/10.1016/j.apenergy.2018.01.086>.
- [19] L. Noltng, A. Praktiknjo, Techno-economic analysis of flexible heat pump controls, *Applied Energy* 238 (2019) 1417–1433. doi:<https://doi.org/10.1016/j.apenergy.2019.01.177>.
- [20] M. Mork, A. Xhonneux, D. Müller, Nonlinear distributed model predictive control for multi-zone building energy systems, *Energy and Buildings* 264 (2022) 112066. doi:<https://doi.org/10.1016/j.enbuild.2022.112066>.
- [21] I. T. Michailidis, T. Schild, R. Sangi, P. Michailidis, C. Korkas, J. Fütterer, D. Müller, E. B. Kosmatopoulos, Energy-efficient hvac management using cooperative, self-trained, control agents: A real-life german building case study, *Applied Energy* 211 (2018) 113–125. doi:<https://doi.org/10.1016/j.apenergy.2017.11.046>.
- [22] P. Zwickel, M. Frahm, J. Galenzowski, K.-H. Häfele, H. Maaß, S. Waczowicz, V. Hagenmeyer, Demand response in smart districts: Model predictive control of building cooling, in: 2022 IEEE PES Innovative Smart Grid Technologies Europe (ISGT-Europe), 2022.
- [23] M. Frahm, S. Meisenbacher, E. Klumpp, R. Mikut, J. Matthes, V. Hagenmeyer, Multi-Zone Grey-Box Thermal Building Identification with Real Occupants, in: 9th ACM International Conference on Systems for Energy-Efficient Buildings, Cities, and Transportation, BuildSys'22, Association for Computing Machinery, 2022. doi:10.1145/3563357.3567403.
- [24] H. Madsen, J. Holst, Estimation of continuous-time models for the heat dynamics of a building, *Energy and Buildings* 22 (1) (1995) 67–79. doi:[https://doi.org/10.1016/0378-7788\(94\)00904-X](https://doi.org/10.1016/0378-7788(94)00904-X).
- [25] IDM Energiesysteme GmbH, Aero slm luftwärmepumpe - idm energiesysteme gmbh (2020). URL <https://www.idm-energie.at/aero-slm-luftwaermepumpe/>
- [26] ANSI/ASHRAE, Standard 55, Thermal Environmental Conditions for Human Occupancy (2017).
- [27] ISO, 7730 - Ergonomics of the thermal environment — Analytical determination and interpretation of thermal comfort using calculation of the PMV and PPD indices and local thermal comfort criteria (2005).
- [28] CEN, EN 16798-1 - Energy performance of buildings - Ventilation for buildings. Part 1: Indoor environmental input parameters for design and assessment of energy performance of buildings addressing indoor air quality, thermal environment, lighting and acoustics (2019).
- [29] P. O. Fanger, Thermal Comfort Analysis and Applications in Environmental Engineering, McGraw-Hill, New York, 1970.
- [30] F. Tartarini, S. Schiavon, T. Cheung, T. Hoyt, Cbe thermal comfort tool: Online tool for thermal comfort calculations and visualizations, *SoftwareX* 12 (2020) 100563. doi:<https://doi.org/10.1016/j.softx.2020.100563>.
- [31] M. Frahm, F. Langner, P. Zwickel, J. Matthes, R. Mikut, V. Hagenmeyer, How to Derive and Implement a Minimalistic RC Model from Thermodynamics for the Control of Thermal Parameters for Assuring Thermal Comfort in Buildings, in: Open Source Modelling and Simulation of Energy Systems (OSMSSES), IEEE, 2022. doi:10.1109/OSMSSES54027.2022.9769134.
- [32] V. Hagenmeyer et al., Information and communication technology in energy lab 2.0, *Energy Technology* 4 (1) (2016). doi:<https://doi.org/10.1002/ente.201500304>.
- [33] Entso-e transparency platform (21.07.2022). URL <https://transparency.entsoe.eu/>
- [34] Y. Peng, A. Rysanek, Z. Nagy, A. Schlüter, Using machine learning techniques for occupancy-prediction-based cooling control in office buildings, *Applied Energy* 211 (2018) 1343–1358. doi:<https://doi.org/10.1016/j.apenergy.2017.12.002>.

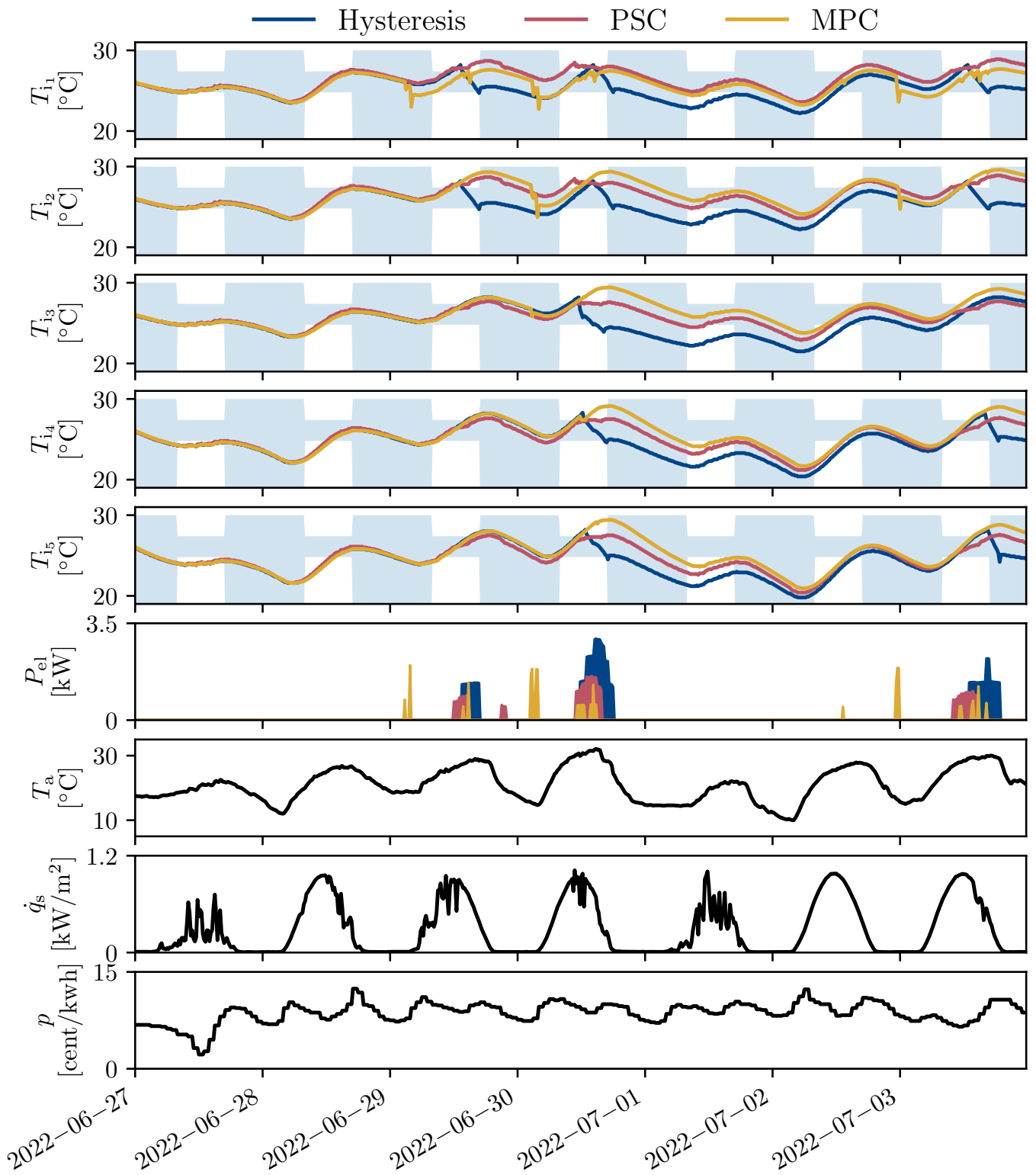


Figure A.5: Control results for three different controllers in the (a) base scenario over a period of one week